COBEM 2023 27TH INTERNATIONAL CONGRESS OF MECHANICAL ENGENEERING

ABCM Brazilian Society of Mechanical Sciences and Engineering
27th ABCM International Congress of Mechanical Engineering
December 04-08, 2023, Florianópolis-SC, Brazil

COB-2023-0293
A COMPARISON OF DROPLET BREAKAGE IN W/O EMULSION FLOW INDUCED BY PUMPING AND GAS PRESSURIZATION

Murilo Zucatelli Elias
Ligia Gaigher Franco
Rayane Reinholz Boone Corona
Edimilson Kempin Júnior
Juliana Thomes Alves Roberti
Rogerio Ramos

Universidade Federal do Espírito Santo – UFES. Av. Fernando Ferrari, 514, Campos Universitário de Goiabeiras, Vitória ES, CEP 29075-910, Brazil

murilozucatelli@gmail.com, ligiagaigherf@gmail.com, rayane.boone@gmail.com, edimilsonkj@gmail.com, juliana_thomes@hotmail.com, rogerio.ramos@ufes.br

Abstract. *In deepwater oil exploration, stable water-in-oil emulsions form due to the process of pumping from the production well to the platform. Therefore, the aim of this work is to present the behavior of the Droplet Size Distribution (DSD) of water-in-oil (W/O) metastable emulsion as it flows through a laboratory-scale experimental flow circuit induced by two distinct methods: compressed air or mechanical pumping. An experimental flow circuit installed in a laboratory scale presents dynamic similarity to the flow of crude oil in offshore installations based on Weber number. The circuit is equipped with pipe fittings that resemble those employed in actual production plants. The dependence of droplet breakage, evaluated by either pressurized or pumped flow, shows variations in DSD in W/O emulsions with concentrations ranging from 7% to 10%. This analysis considers an initial $D_{[4,3]}$ diameter from 10 µm to 25 µm and repeats the tests for each form of flow induction. The results indicate repeatability in the Weber number, ranging from 0.5 to 7, and different characteristics of the initial DSD.*

Keywords: *emulsion, droplet breakage, water-in-oil emulsions, droplet size distributions*

1. INTRODUCTION

In the current scenario of the global energy matrix, the consumption of hydrocarbons could reach 104 mb/d in the year 2026 (IEA, 2021), encompassing the transport sector, energy, and products such as the manufacture of plastics, pharmaceuticals, solvents, etc. Given the importance of this asset, efforts are being made to improve the efficiency of the primary and secondary oil and gas extraction processes, especially for separating oil and water from the emulsion as well as removing sediments. The high shear promoted by valves and pumps, combined with the presence of natural oil emulsifiers such as resins and asphaltenes, leads to the formation of stable emulsions (Van der Zande et al., 1998; Corona et al., 2023).

Given these adversities, the separation of oil and water becomes more expensive in terms of energy, use of chemical products and physical space required by separators equipment. The investigation of emulsion formation from the well to separator vessel is not completely known yet. In this sense, the physical mechanisms that promote droplet breakage are found mainly in choke valves (Van der Zande et al., 1999; Kwakernaak, 2007), submersible pumps, and Wet Christmas Tree (WCT).

Such investigations are carried out through experimental arrangements, with the injection of the liquid-liquid phases separately into inline mixers. From another perspective, the use of a model fluid emulsion, designed with physical-chemical properties similar to crude oil, proves to be adequate to simulate, in a controlled environment, the development of the emulsion similar to emulsions from real processing conditions (Corona et al., 2023), avoiding safety issues as flammability, for instance.

The flow loop used in this paper is described in the work of Kempin et al. (2022). The primary purpose of the test loop is to assess both the localized breakage of drops by tubes and pipe fittings and the combined effects of devices that resemble those commonly presented in offshore oil production systems. The test fluid is a metastable water-in-oil emulsion, fully characterized, which is prepared and recycled in each test round. Therefore, flow induction mechanisms are designed to promote the lowest impact as possible in reducing the droplet sizes before the emulsion reaches the testing section.

In this context, the objective of this work is to compare the impact of the flow induction methods on the droplet size distribution (DSD) of water-in-oil (W/O) emulsions. The assessed methods are mechanical pumping by helical pump and tank pressurization. The experiments are conducted with several flow ranges defined from the Weber number, and two water concentration levels. The DSD is analyzed at the beginning and at the end of the test section, by taking an emulsion sample with the aid of an optimized piece for extracting emulsion from tubing.

1.1 Droplet breakup modeling

The droplet in a continuous phase is subject to normal and tangential stresses that compete with the stress that tries to keep the droplet cohesive (Hinze, 1955, Kolmogorov 1949). To break a drop, an amount of energy must be consumed to firstly deform the drop and then break the film. The Weber number is a dimensionless group that stands for the ratio among the inertial force and interfacial tension amongst phases, it is calculated as Eq. 1.

$$We = \frac{\tau d}{\sigma}, \tag{1}$$

Where τ [N/m²] is the force from the continuous phase, d [m] is the droplet diameter and σ [N/m] is the interfacial tension. The droplet breaks when the critical Weber is exceeded (Duan, 2003).

Although in this work, the flow in the test section is in laminar regime, the flow induced by pump presents complex phenomena of local velocity fluctuations, which may promote the droplet breakage. When a drop is deformed by dynamic pressure forces, the droplet deformation is caused by changes in continuous phase velocity over a distance equal to the size of the drop. In this case, the force τ can be written as $\rho_c V^2$, where V is the slip velocity and ρ_c is the continuous phase density (Hinze, 1955). Assuming that the droplets are initially at rest and then are accelerated without slipping to the terminal flow velocity, the slip velocity can be taken as the average surface velocity. Then, Weber number is rewritten as Eq. 2:

$$We = \frac{\rho_e V_e^2 d}{\sigma}, \tag{2}$$

where ρ_e [kg/m³] is the emulsion density. The Reynolds number of the pipe flow can be expressed as Eq. 3:

$$\mathrm{Re}_e = \frac{\rho_e V_e^2 D}{\mu_e}, \tag{3}$$

where V_e [m/s] is the emulsion mean velocity in the cross sectional area and D [m] is the pipe diameter.

A commonly method to compare the droplet size distribution is by characteristic mean diameters. In this study, it is used the mean diameters of De Brouckere $D_{[4,3]}$ and Sauter $D_{[3,2]}$ to assess the emulsion distribution, parameters that are very useful for evaluating the mean diameter of dispersed liquid drops (Tadros, 2009). From a DSD, a characteristic diameter $D_{[m,n]}$ can be calculated by Eq. 4:

$$D_{[m,n]} = \left(\frac{\sum_{i=1}^{i=m} f_i d_i^m}{\sum_{i=1}^{i=n} f_i d_i^n} \right)^{\frac{1}{m-n}}, \tag{4}$$

where f_i represents the number frequency of droplets within the range from d_i to d_{i+1}, this characteristic diameter can be directly derived from the laser diffraction analysis. On the other hand, the characteristic diameter evaluated in the cumulative distribution is useful for the analysis of the stable diameter (D_{max}), in this case, D_{v90} is considered, representing the volume in which 90% of the total droplet volume is contained up to that diameter in a distribution based on the volumetric frequency.

2. MATERIALS AND METHODS

2.1 Emulsion description

The emulsions are prepared in the emulsion lab at the Research Group for Oil and Gas Flow and Measurement (NEMOG, in Portuguese), at Federal University of Espírito Santo (UFES). They are composed of mineral oil (Mobil AW-68) with surfactant as continuous phase and saline water (35 g/L NaCl) as dispersed phase. In this work, the water

volumetric concentrations are 7% and 10%. Each test requires 400 L of emulsions. Thus, the characterization of the emulsion is an important process.

The density ρ_e is measured in a temperature range between 20°C and 50°C using the digital densimeter Anton Paar DSA5000M, following ASTM D5002 (2005). The viscosity μ_e is evaluated using double gap coaxial cylinder geometry at 25°C and 35°C using the rheometer HAAKE MARS 60, according to ASTM D4402. The interfacial tension σ between oil and water is obtained by the pendant drop method using the Tensiometer SEO (Phoenix model MT).

For each emulsion sample, water volumetric concentration is measured by potentiometric titration, according to ASTM D4377, using Karl Fischer reagent in a Metrohm titrator (model 836 Titrando).

The emulsion properties are given in Table 1.

Table 1. Emulsion properties.

Property	7% H_2O	10% H_2O
Density [kg/m³]	866	874
Dynamic viscosity [cP]	123	137
Interfacial tension [mN/m]	2.5	2.5

Photomicrographs on a glass slide are produced to check the size and shape of water droplets. An optical microscope with polarized light performs the image acquisition. Figure 1 (a) shows an image for the emulsion sample with 10% v/v of H_2O in the middle level of the supply tank.

The second method used to measure droplet sizes is laser diffraction technology (Betterziser, model ST). The equipment measures the droplet size distribution of W/O emulsions between 0.1 and 1000 µm. Isoparaffin is used as dispersing medium. Figure 1 (b) shows the distribution of three samples obtained in the emulsion storage tank, obtained after fluid homogenization.

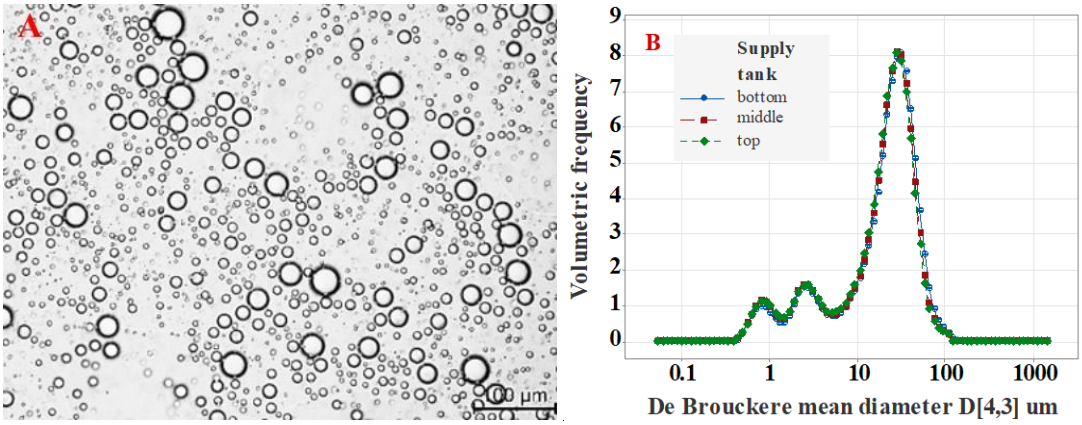

Figure 1. Water-oil emulsion with 10% v/v H_2O in supply tank. (a) Photomicrography. (b) Volumetric frequency distribution.

2.2 Experimental setup

The process and instrumentation diagram (P&ID) of the flow loop is shown in Figure 2. A 500 L emulsion tank (TK-01) is used for emulsion storage, homogenization and sampling. It fills a 750 L pressure vessel (TK-02) before experimental startup by gravity. The pressure vessel TK-02 is equipped with pressure sensors (PT-01, Warme WTP 4010), temperature sensor (TT-01, Zurich T.420.I.H) and compressed air supply from a 30 hp screw compressor (C-01, Chiaperini COPA 30 G2). A globe valve (PCV-01, Samson 3241) controls the compressed air supply.

Flow can be promoted by two methods. The first one is mechanical pumping, using the helical pump P-01 (Helibombas, 2HT-32), driven by a 4 HP electric motor coupled to a variable speed drive (WEG CFW500). In this case, valves HV-03 and HV-05 are opened and all others are remained closed.

The second method is by pressurizing TK-02, with is half filled with emulsion, with compressed air, and opening valves SV-01 and HV-4 (with other valves closed). Thus, pump P-01 is bypassed. The pressure control valve PCV-01 controls the air entrance in order to achieve and maintain the desired flow rate.

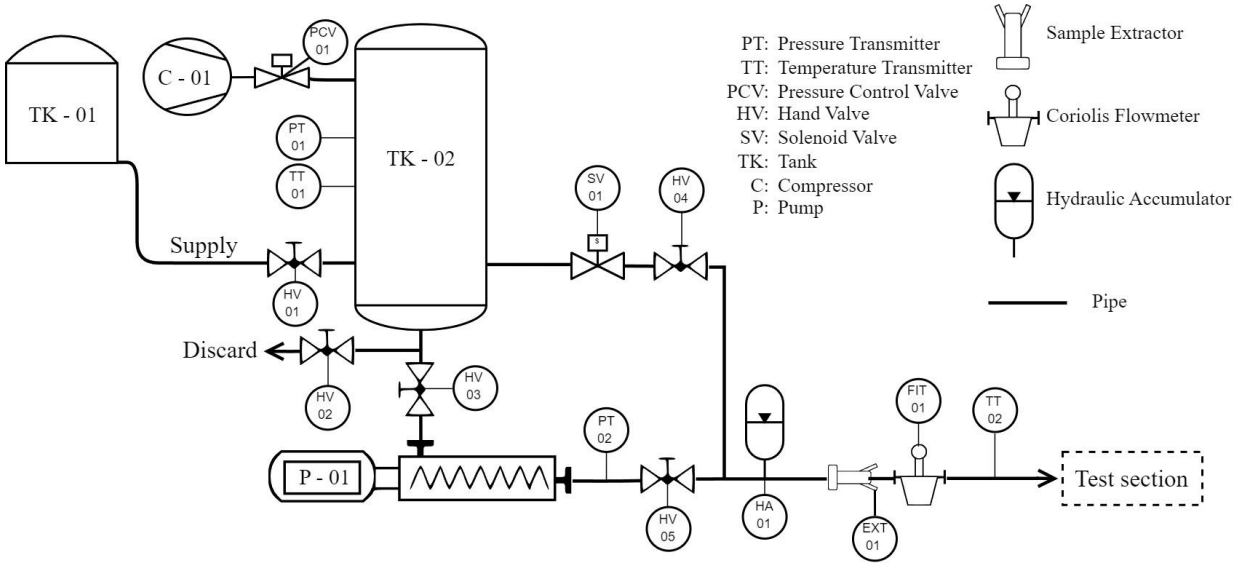

Figure 2. Schematic diagram of the emulsion flow loop.

The flow rate is measured by the Coriolis flowmeter FIT-01 (MicroMotion 2700). The pressure sensor PT-01 (Warme TP7196) measures the pressure in the vessel TK-02 and the pressure sensor PT-02 (Microsensor M20) measures pressure at the pump outlet. After the Coriolis flowmeter, fluid temperature is measure by the sensor TT-02 (Zurich T.420.I.H). Additionally, the flow circuit includes a hydraulic accumulator (HA-01, Ciltech) to attenuate pump pressure fluctuations.

The emulsion is sampled in the flowline through extractor devices (EXT-01 among others installed along the test section). These special pieces are 3D printed, resin made and are used to evaluate the droplet size distribution before and after pipe fittings. Tubes are stainless steel made, with internal diameter of 21 mm.

Data acquisition and plant control are integrated into a supervisory system based on the LabView platform.

2.3 Experimental procedure

The emulsion batch is prepared following the methodology of Corona et al. (2023), adapted to produce emulsions with 7% and 10% of water volumetric concentration. For the increase of dispersed phase, it is necessary a smooth homogenization, so that the emulsion is metastable.

The emulsion stored in tank TK-01 is sampled at three levels of the tank: surface, middle and bottom. These samples are conducted to laser diffraction analysis in order to obtain the droplet size distribution. In this sense, the original DSD is taken as the average DSD of these three samples.

After sampling, TK-01 is lifted, so that the emulsion smoothly flows to the pressure vessel TK-02 by gravity. This filling procedure aims to maintain the original DSD in the tests. The time period between complete filling and the start of flow test does not exceed 30 minutes, which is a period shorter than the separation period for the emulsion with 10% of water reported by Corona et. al. (2023).

After flow starts, the first emulsion sample takes place after 1 minute after stabilization of flow rate and pressure readings, ensuring complete renewal of the fluid within the flow loop and extractor devices as well. A emulsion sample is taken immediately for DSD analysis in order guarantee that the characteristics of the sample are maintained.

2.4 Experimental conditions

The experimental test matrix was designed by a full factorial experiment (Montgomery, 2010), with two levels of water concentration, two levels of fluid induction method and eight levels of Weber number. The water volumetric concentrations are 7% and 10% v/v of H_2O. The Weber numbers are: 0.5, 1, 2, 3, 4, 5, 6 and 7. Table 2 summarizes the experimental conditions.

Table 2. Experimental conditions.

Test code	Induction method	% H_2O	Weber number	Number of tests
A	Pressurized vessel	7	0.5 to 7	2
B	Pump	7	0.5 to 7	2
C	Pressurized vessel	10	0.5 to 7	2
D	Pump	10	0.5 to 7	2

Although the temperature of emulsions is not a controlled, the test runs was performed at 28.5°C.

The flow test starts at the lowest flow rate, which corresponds to the lowest Weber number of 0.5. After 1 minute, an emulsion sample is taken. Then, the flow rate is increased to the next Weber level, waiting for the fluid renewal in the system, and then a new emulsion sample is taken. This procedure repeats until the last Weber level is reached.

For each sample, the DSD analysis is performed both by laser diffraction method and photomicroscopy. These analyses are done three times for each sample, in order to check possible random error, besides ensuring the repeatability of results. For each emulsion sample, the DSD is adopted as the average of the laser diffraction analysis of three samples, and the variability of the DSD is obtained from the standard deviation of these analyses.

3. RESULTS AND DISCUSSION

The emulsion sampled in the storage tank, before the beginning of flow, is considered with Weber number equal to zero. Figure 3 illustrates the average $D_{[4,3]}$ in flows induced by pump and by tank pressurization, water volumetric concentration of 7% and 10%. The average $D_{[4,3]}$ is calculated based on the six measurements, three measurements for each experimental condition. The $D_{[4,3]}$ variability of the experimental condition is a root mean square of one standard deviation of each test replicates, normalized by the average $D_{[4,3]}$. This characteristic diameter is commonly used to calculate Weber dimensionless number as in Eq. (2).

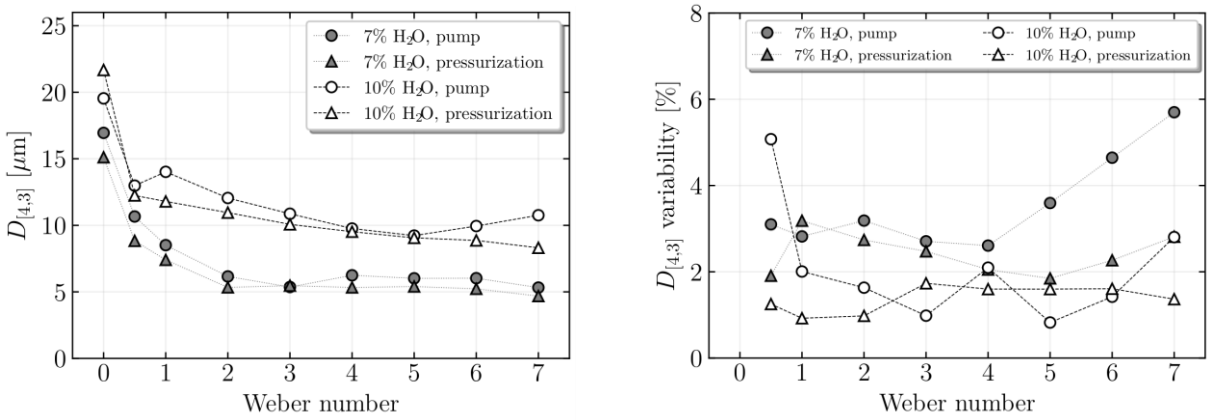

(a) (b)

Figure 3. (a) Average $D_{[4,3]}$ evaluated downstream to the pump and pressure tank (EXT-01) for concentrations of 7 and 10% H_2O v/v. (b) Variability of $D_{[4,3]}$.

For both H_2O volume fractions, there is a noticeable reduction in $D_{[4,3]}$ with an increase of Weber number, especially for Weber below 2. At 7% H_2O, a stabilization of $D_{[4,3]}$ is observed in Weber numbers above 2. In this case, the average droplet diameter is higher in pump-induced flow of 5.86 μm, against 5.2 μm in pressure-induced flow. In general, the $D_{[4,3]}$ variability is higher in pump-induced flow at 7% H_2O, when compared with pressure-induced flow, with variabilities ranging from 2.6% (We = 4) to 5.7% (We = 7). The results for testes with 7% H_2O conducted by pressurization show $D_{[4,3]}$ variability between 1.8% (We = 5) and 3.2% (We = 1).

For H_2O volume fractions of 10%, there is a slight difference in $D_{[4,3]}$ conducted by pump and pressurization, with the mean droplet diameter being higher for pump-induced tests. This behavior is similar to what is observed in emulsions with 7% H_2O. For We > 3, the average $D_{[4,3]}$ stabilizes around 10.11 μm for pump-induced tests and around 9.17 μm for pressure-induced tests. In general, the variability of $D_{[4,3]}$ is higher in pump-induced tests, ranging from 0.8% (We = 5) to 5.1% (We = 0.5). In pressure-induced tests, the variability ranges from 0.9% (We = 1) to 1.7% (We = 3). In pump-induced flow with 10% of H_2O at We = 0.5, the average diameter is slightly lower than at We = 1.0. The profile of decay of DSD with the increase of Weber remains.

Regarding the type of flow induction, the difference in the distributions is not statistically significant when increasing volumetric concentration from 7% to 10% and Weber number from 0.5 to 7 for both flow induction methods: pumping or pressurization. Across a total of 32 experimental points analyzed for each induction method, with the increase of water concentration, the average $D_{[4,3]}$ increases 53.1% for the test induced by pump and 63.2% for the test induced by gas pressurization.

The ANOVA method is used to evaluate the contribution of factors in the experiments and return the main effects that contribute to the variation in the average diameter $D_{[4,3]}$. Figure 4 illustrates the effects of various factors, including concentration, type of flow induction, and Weber number. The Pareto diagram provides a summary of the most significant factors, condensing the method for assessing the magnitude of these effects. The size of these effects is evaluated based

on the difference between the highest and lowest means. An effect with a substantial impact (>2) is represented in red, while an effect with a minor impact (<1) is indicated in gray.

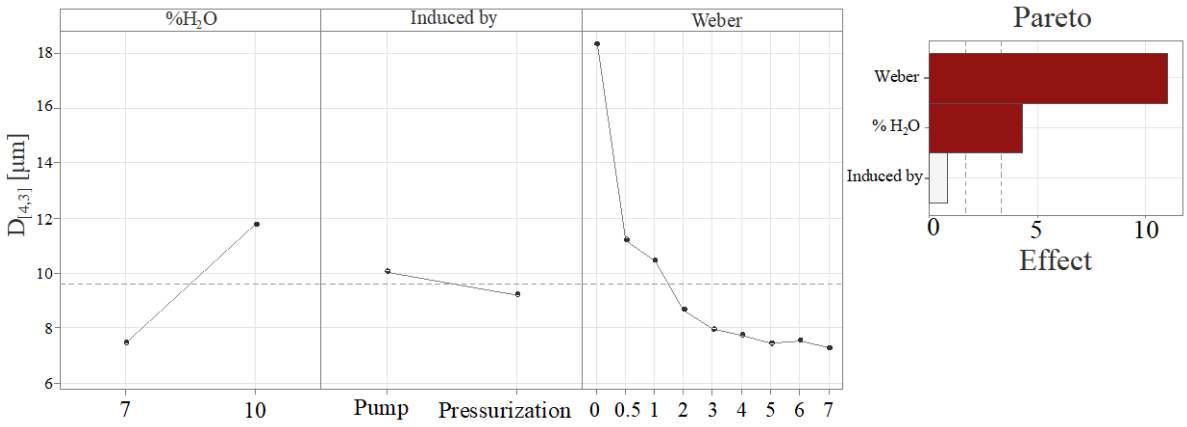

Figure 4. Main effects and Pareto diagram for $D_{[4,3]}$ for water concentration, induced type and Weber number.

The type of flow induction has a relatively minor effect compared to other factors. The specific pump employed has the potential for a smaller impact on reducing emulsion droplet size. The dispersed phase concentration has a lesser effect than the evaluated Weber number, primarily due to the limited range of evaluation when compared to the achievable limit (20% water).

Figure 5 illustrates the behavior of the global average dimensionless droplet diameter for each flow induction methods, taking into account the volumetric concentrations of the dispersed phase and the evaluated Weber numbers. The We = 0 is ignored in the analysis, but it is used to dimension $D_{[4.3]}$ and make the averages independent of the initial flow condition. Therefore, the results represent the overall percentage reduction in the average droplet size.

In both cases, the results for flow induced by the pump tend to promote a less droplet breakup when compared to the pressure-induced flow. However, given the uncertainty in the DSD analysis, it is possible to obtain a similar DSD for the same flow induced by tank pressurization. Nevertheless, a one-way ANOVA analysis at a significance level of 5% indicates that this difference is not statistically significant.

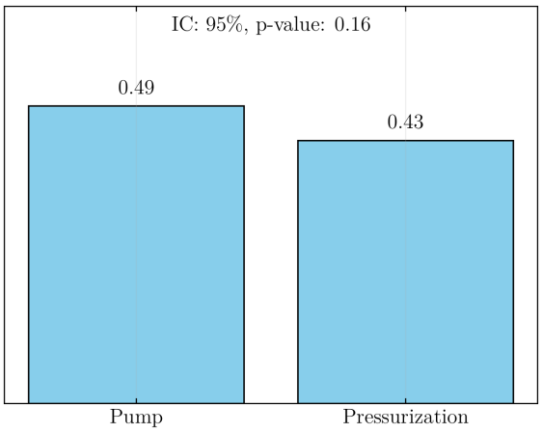

Figure 5. Global dimensionless average $D_{[4.3]}$ evaluated downstream of the pump and pressure tank (EXT-01). The values are normalized by the average $D_{[4.3]}$ in the tank (We = 0).

It can be concluded that both pumping flow and pressurized vessel provide energy to the emulsion. Although with low shear, it is found that the droplet breakup phenomenon occurs for Weber above 0.5, independently of the initial mean droplet size. The concentration of the dispersed phase has a notable effect and is significant within the range of water concentration evaluated.

An estimation of the maximum stable droplet diameter through the characteristic diameter D_{v90} is obtained and illustrated in Figure 6. The droplet size corresponding to 90% of the cumulative volume (D_{v90}) is adopted to represent D_{max}. The shear applied by the pump to the emulsion leads to a reduction in the maximum diameter, resulting in a diameter which is equal to or greater for We > 3.0, when compared to the other induction method.

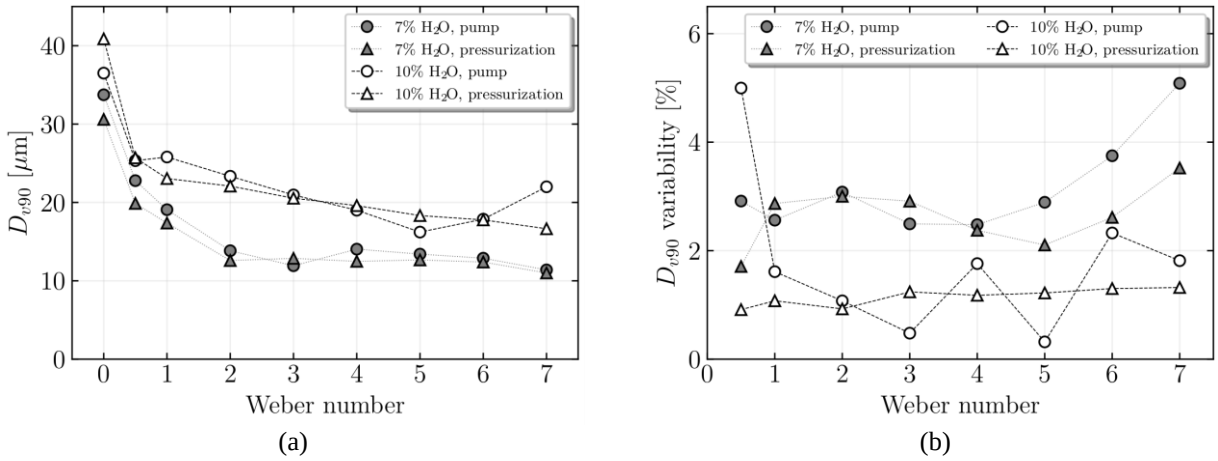

Figure 6. (a) Average D_{v90} evaluated downstream to the pump and pressure tank (EXT-01) at a concentration of 7 and 10% H_2O. (b) Variability of D_{v90}.

Following the same trend as presented for $D_{[4,3]}$, for both H_2O volume fractions, there is a noticeable reduction with an increase in Weber number, until Weber reaches 3. In the case of 7% H_2O, the average droplet diameter is higher in pump-induced flow, measuring 14.9 µm, compared to 13.9 µm in pressure-induced flow. In general, the D_{v90} variability is higher in pump-induced flow at 7% H_2O, when compared with pressure-induced flow, with variabilities ranging from 2.48% (We = 4) to 5.1% (We = 7). The results for tests conducted by pressurization show D_{v90} variability between 1.7% (We = 0.5) and 3.5% (We = 7).

For 10% H_2O and flow induced by pressurization, the reduction of D_{v90} is continuous with the increase in Weber, reaching a 59.3% reduction from the initial average size when it reaches We = 7. Similarly, for 10% H_2O, the lowest variability in results was observed for any of the induction types. The average droplet diameter is also higher in pump-induced flow, measuring 21.3 µm, compared to 20.46 µm in pressure-induced flow, excluding We = 0. In general, the D_{v90} variability is higher in pump-induced flow as well, with variabilities ranging from 0.3% (We = 5) to 5% (We = 0.5). The results for tests conducted by pressurization show D_{v90} variability between 0.9% (We = 0.5) and 1.3% (We = 7).

Schmitt (2021) and other authors uses D_{v95} to represent D_{max}. Dabirian (2018) applies a linear correlation to find $D_{[3,2]}$ from D_{max}, $D_{[3,2]} = 0.4D_{max}$. The cited authors use this model to evaluate shear effect models in pumps. Nevertheless, the test results indicate that the dependence of D_{max} on $D_{[4,3]}$ is linear, with a Pearson correlation coefficient of 0.99 and a confidence interval ranging from 0.98 to 1.0. Figure 7 illustrates other correlations using the Pearson method.

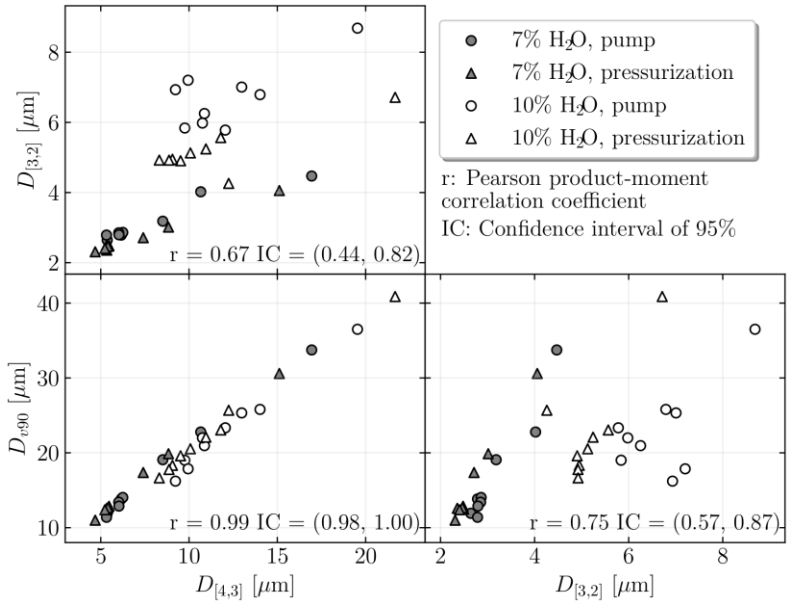

Figure 7. Pearson correlation between characteristic diameters commonly used in literature.

The maximum stable droplet size decreases as rotational speeds increase, i.e., with the increase in emulsion flow rates. This result is consistent with the findings in the work of Perissinotto et al. (2020), where the authors associated the

maximum stable droplet size with centrifugal forces and higher emulsion velocities, which intensify disruptive stresses and interfacial forces. Therefore, as previously discussed for $D_{[4,3]}$, the estimation of the maximum stable droplet diameter must take into account the emulsion properties and the velocity fluctuations (Hinze, 1955).

Considering that disturbances in DSD caused by emulsion sampling are evaluated and minimized in this study, it becomes evident that some of the high variability observed in emulsions sampled in EXT-01 and what is measured in a quiescent fluid at the end of the test section is not statistically significant.

4. FINAL REMARKS

This study presented an experimental investigation on the droplet size distribution in the flow of water-in-oil emulsions induced by pump and induced by tank pressurization. The dimensionless number of Weber is used to interpret the experimental data and to ensure dynamic similarity between tests. The results show the feasibility of the system operating with mechanical pumping using a helical pump, ensuring an equal or lower DSD reduction for the mean and maximum droplet diameter when compared to the flow induced by tank pressurization.

Regarding $D_{[4,3]}$, the results show that pump-induced flows promote less droplet breakage, as indicated by the higher $D_{[4,3]}$. Additionally, it is not possible to correlate $D_{[4,3]}$ variability with the Weber number. The greatest variability was observed at the lowest and highest Weber values.

The ANOVA analysis reveals that pump-induced flows have a weaker effect compared to volumetric concentration and Weber number. Pump flow tends to maintain stable maximum diameter similar to that of pressurization. Furthermore, D_{max} follows the same trend as $D_{[4,3]}$, with greater variability observed at the smallest and largest Weber numbers. D_{v90} and $D_{[4,3]}$ exhibit a much higher correlation compared to $D_{[3,2]}$ and D_{v90} (or D_{v95}), which are commonly used in the literature.

One can conclude that the reduction in droplet size observed in pressurized induced flow compared to pump-induced flow may be associated with the pipe fittings connecting the outlet of the pressure vessel with the test section. A future study should focus on establishing a correlation between the mean energy dissipation rate within the pump, using the methodology developed by Schmitt et al. (2021) for centrifugal pumps and adapting it for the helical pump. Such an investigation will enable the evaluation of droplet size models in pumps designed to handle water-in-oil dispersions.

5. ACKNOWLEDGEMENTS

The authors thank Laboratory of Research and Methodologies Development for Petroleum Analysis (LabPetro/UFES) for using the photomicrography equipment and determining the water content, as well as the chemistry team for their commitment and determination in preparing the emulsion as well as in determining the droplet size distribution.

The authors thank Laboratory of Experimental Methods in Transport Phenomena (LaMEFT/UFES) for granting the use of the rheometer to determine the viscosity of the emulsion.

The authors would like express their gratitude to Petróleo Brasileiro Company (Petrobras) and Agência Nacional do Petróleo, Gás Natural e Bio Combustíveis (ANP) by the financial support through grant 2018/00482-9.

6. REFERENCES

American Society for Testing and Materials. (2005). ASTM D5002: Standard Test Method for Density and Relative Density of Crude Oils by Digital Density Analyzer.

American Society for Testing and Materials. (2006). ASTM D4377: Standard Test Method for Water in Crude Oils by Coulometric Karl Fischer Titration.

American Society for Testing and Materials. (2015). ASTM D4402: Standard Test Method for Measuring the Viscosity of Mold Powders above Their Melting Point Using a Rotational Viscometer.

Corona, R. R., Sad, C. M., da Silva, M., de Castro, E. V., Quintela, E. F., & Ramos, R. (2023). Selecting a model fluid with properties similar to crude oil to test the formation of W/O emulsions. Geoenergy Science and Engineering, 221, 111265.

Dabirian, R., Cui, S., Gavrielatos, I., Mohan, R., & Shoham, O. (2018, July). Evaluation of models for droplet shear effect of centrifugal pump. In Fluids Engineering Division Summer Meeting (Vol. 51555, p. V001T06A014). American Society of Mechanical Engineers.

Duan, Ri-Qiang, Seiichi Koshizuka, and Yoshiaki Oka.: Numerical and theoretical investigation of effect of density ratio on the critical Weber number of droplet breakup. Journal of nuclear science and technology 40.7 501–508 (2003).

Hinze, J. O. (1955). Fundamentals of the hydrodynamic mechanism of splitting in dispersion processes. AIChE journal, 1(3), 289-295.

IEA. Oil 2021: Analysis and forecast to 2026. Paris, 2021.

Kempin Jr, E., Roberti, J. T., Franco, L. G., & Ramos, R. (2022). Engineering Aspects on Flow Similarity for Design Water-in-oil Emulsion Circuit. In Multiphase Flow Dynamics: A Perspective from the Brazilian Academy and Industry (pp. 255-265). Cham: Springer International Publishing.

Kolmogorov, A. On the disintegration of drops in a turbulent flow. Dok. Akad. Nauk 1949, 66, 825–828.
Kwakernaak, P. J., van den Broek, W. M., & Currie, P. K. (2007, March). Reduction of oil droplet breakup in a choke. In Production and Operations Symposium. OnePetro.
Montgomery, Douglas C.; RUNGER, George C. Applied statistics and probability for engineers. John wiley & sons, 2010.
Paiva, A.P., 2004. Estudo da minimização de erro das medições de concentração de emulsões por titração Karl–Fisher utilizando-se projetos de experimentos. Universidade Federal de Itajubá, RJ, Brazil (Master's thesis).
Perissinotto, R. M., Verde, W. M., Perles, C. E., Biazussi, J. L., de Castro, M. S., & Bannwart, A. C. (2020). Experimental analysis on the behavior of water drops dispersed in oil within a centrifugal pump impeller. Experimental Thermal and Fluid Science, 112, 109969.
Schmitt, P., Sibirtsev, S., Hlawitschka, M. W., Styn, R., Jupke, A., & Bart, H. J. (2021). Droplet Size Distributions of Liquid-Liquid Dispersions in Centrifugal Pumps. Chemie Ingenieur Technik, 93(1-2), 129-142.
Tadros, T. F. (2009). Emulsion science and technology: a general introduction. Emulsion science and technology, 1(1), 1-55.
Van der Zande, M. J., Van Heuven, K. R., Muntinga, J. H., & Van den Broek, W. M. G. T. (1999, October). Effect of flow through a choke valve on emulsion stability. In SPE Annual Technical Conference and Exhibition. OnePetro.
Van der Zande, Mark J., and W. M. G. T. Van den Broek: Breakup of oil droplets in the production system. Proceedings of ASME Energy Sources Technology Conference and Exhibition, Houston. (1998).

7. RESPONSIBILITY NOTICE

The authors are the only responsible for the printed material included in this paper.